Impaired Autophagic Activity Contributes to the Pathogenesis of Bronchopulmonary Dysplasia: Evidence from Murine and Baboon Models

Liang Zhang, Sourabh Soni, Elvin Hekimoglu, Sara Berkelhamer, and Sule Çataltepe

Online Data Supplement

Materials and Methods

Murine model of neonatal hyperoxia-induced lung injury

Becn1$^{+/-}$ mice were obtained from Dr. Beth Levine (University of Texas Southwestern Medical Center at Dallas, Dallas, Texas, USA) and *GFP-LC3* mice were obtained from Dr. Noboru Mizushima (University of Tokyo, Tokyo, Japan). Wild-type C57BL/6 littermates were used as controls for *Becn1*$^{+/-}$ mice. *Becn1*$^{+/-}$ mice were identified by coat color and PCR-based genotyping from tail tips. All procedures performed on mice were approved by the Animal Care and Use Committee at Brigham and Women's Hospital.

Within 12 hours of birth, pups from 2 litters were randomly and evenly distributed among the newly delivered dams (6-7 pups/dam). One-half of the pups were exposed to 75% oxygen in a controlled atmosphere animal chamber (Biospherix, NY, USA), while the other half were exposed to room air (RA) as previously described (1). Oxygen concentration in the chamber was maintained using ProOx O_2 controller (Biospherix). Nursing mothers were rotated between the oxygen-exposed and RA litters every 24 hours to avoid oxygen toxicity in the mothers and to eliminate maternal effects between the groups. Pups were sacrificed on P0.25, P0.5, P1, P3, P5, P7, P10 or

P14.

Baboon model of BPD

The frozen baboon lung tissue samples were provided by the Southwest Foundation for Biomedical Research (San Antonio, TX, USA). All procedures performed on baboons were reviewed and approved by the Animal Care and Use Committees of the Southwest Foundation for Biomedical Research and the University of Texas Southwestern Medical Centre. For the BPD model, premature baboons were delivered by hysterotomy at 125 days after receiving antenatal steroid treatment. They were intubated, treated with exogenous surfactant (Survanta; donated by Ross Laboratories, OH, USA) and maintained on pressure-limited, time-cycled infant ventilators (donated by Infant Star; Infrasonics, CA, USA) for 14 days. The ventilator settings were adjusted to maintain the arterial carbon dioxide tension (PaCO2) between 45 and 55 mmHg while oxygen was provided on a PRN basis to maintain the arterial oxygen tension (PaO2) between 55 and 70 mmHg. Animals that were sacrificed at 14 days had pathologic and biochemical findings that were characteristic of the new BPD seen in human infants as described previously (2, 3). Baboons that were delivered at 140 days and euthanized before the first breath served as the gestational controls.

In the old BPD model, baboons were delivered at 140 d gestation (the equivalent of ~29-30 weeks and were ventilated for a total of 10 d with 100% oxygen (4).

Human tracheal aspirate samples

Human tracheal aspirate (TA) samples were obtained during routine care of intubated preterm infants as discarded samples with an exempt protocol that was approved by Brigham and Women's Hospital Institutional Review Board. Cytospins were prepared from TA samples within 30 minutes of collection.

Harvesting and processing of murine lung tissues

Following euthanasia, lungs were perfused with PBS through the right ventricle. Both lungs were removed, snap frozen in liquid nitrogen and stored in -80˚C. In other cohorts of mice, lungs were inflated with 10% neutral buffered formalin at a constant pressure of 25 cm H_2O and stored in the same fixative overnight and fixed lung tissues were transferred to 75% ethanol or 30% sucrose the next morning for paraffin or OCT embedding, respectively.

Bronchoalveolar lavage (BAL), isolation and culture of murine alveolar macrophages

BAL was performed on 7d-old mouse pups. Trachea was cannulated with a 24 G angiocath and lungs were lavaged with 0.3 ml ice cold Mg^{2+}- and Ca^{2+}-free PBS 5 times. The lavages were combined and centrifuged at 200 g for 10 minutes at 4˚C. The supernatant was stored at -80˚C. The BAL cells were resuspended in PBS and enumerated using a hemocytometer. Differential cell counts were performed on cytocentrifuge preparations stained with Diff-Quik stain. Equal numbers of resuspended BAL cells were seeded in 24-well plates with RPMI media and were cultured in 5% CO_2 incubator at 37˚C for 2 h. Non-adherent cells were removed by washing the dishes three times with sterile PBS. The attached alveolar macrophages were scraped down and used for RNA extraction (5).

Morphometric analysis

5 μm thick paraffin-embedded lung sections were stained with modified Gill's stain for measurements of mean linear intercept (MLI), as a surrogate for alveolar diameter, or hematoxylin and eosin (H&E) for assessment of general architecture and measurements of alveolar septal thickness. Lung sections were viewed under a Nikon Eclipse 80*i* microscope (Nikon, Tokyo,

Japan) and 4-6 images of lung parenchyma from each pup were captured at 200 × magnification using NIS-Elements Basic Research software. Image acquisition and analyses were performed by investigators blinded to the groups. MLI measurements were initially done using NIH ImageJ software and then confirmed by manual measurements on a subset of samples as previously described (6). Alveolar septal thickness measurements were performed using NIS-Elements Basic Research software (Nikon).

Antibodies

Sources and dilutions of primary antibodies used in immunofluorescence (IF) and Western blot (WB) analyses are listed in Table E1. Secondary antibodies used for WB were anti-mouse or anti-rabbit IgG-horseradish peroxidase (HRP) raised in horse and goat, respectively (Table E2). Secondary antibodies used for IF were Alexa Fluor® 594 goat anti-mouse or anti-rabbit IgG and Alexa Fluor® 488 goat anti-mouse or anti-rabbit IgG (Invitrogen, MA, USA).

Immunostaining of mouse lung sections

Double immunofluorescence staining was performed as previously described (7, 8). Briefly, lung sections were deparaffinized and after blocking and antigen retrieval in citrate pH 6 buffer at 95

˚C for 15 min, they were incubated with primary antibodies overnight and with secondary antibodies for 1 h at room temperature. After washing in PBS, sections were mounted in Vectashield (Vector Laboratories) and viewed under a Nikon Eclipse 80*i* microscope. Images were captured using NIS-Elements Basic Research software.

RNA extraction and quantitative reverse transcriptase polymerase chain reaction (qRT-PCR)

Total RNA was extracted from adhesion purified alveolar macrophages using RNeasy mini kit (Qiagen, Germany) following the manufacturer's instructions. Briefly, cell lysis was performed using RLT lysis buffer containing β-mercaptoethanol and the homogenate was then centrifuged at 12,000 *g* for 3 min in a 4°C centrifuge. This was followed by an addition of equal volume of 70% ethanol to the supernatant; the mixture was then loaded to the RNeasy mini spin column and centrifuged at 12,000 *g* for 1 min at 4°C. RW1 and RPE buffers were then employed for column washing and finally RNA was eluted in nuclease-free water. Quantification of extracted RNA was performed on NanoDrop 2000C spectrophotometer (Thermo Fisher Scientific, MA, USA). Extracted RNA was used for complementary DNA (cDNA) synthesis using High-Capacity RNA-

to-cDNA Kit (Applied Biosystems, MA, USA). qRT-PCR amplification assays were performed using Green-2-Go qPCR Mastermix-ROX (Bio Basic, NY, USA). All Primer sets were custom synthesized and obtained from Integrated DNA Technologies, IA, USA (Table E3). The thermal cycling protocol employed is as follows: 95°C for 10 min (enzyme activation), followed by 40 cycles of denaturing at 95°C for 15 sec, annealing and extension at 60°C for 60 sec and a standard melt curve in an automated sequence detection system (StepOnePlus Real-Time PCR System, Applied Biosystems, MA, USA). Relative gene expression was obtained after normalization with endogenous expression of mouse 18sRNA and fold change in gene expression was calculated using the comparative threshold $2^{-\Delta\Delta C_t}$ method. All qRT-PCR assays were performed at least three times.

Western blotting

For protein expression analysis, mouse and baboon lung tissues were homogenized in RIPA lysis buffer (Boston Bio Products, MA, USA) containing 1 tablet protease inhibitor cocktail (Thermo Fisher Scientific, MA, USA) per 10 ml in a Dounce homogenizer. After centrifugation at 12,000 *g* for 10 minutes, total protein content in the supernatant was determined using the Pierce BCA

Protein Assay Kit (Thermo Fisher Scientific). Equal amount of protein samples were added into 4× Laemmli's-SDS sample buffer followed by boiling at 95°C for 5 min and resolved by SDS-polyacrylamide gel electrophoresis (12.5 % acrylamide), and proteins were transferred from the gels to nitrocellulose (Amersham, GE Healthcare, IL, USA) or PVDF (used only for LC3, Invitrogen, MA, USA) membranes. 5% non-fat dried milk was used to block the membrane for 1 h at room temperature followed by probing with specific primary antibodies overnight at 4°C. The membrane was washed by 1x PBST and incubated with secondary antibody for 1 h at room temperature. β-actin was used as an internal loading control to normalize the protein expression. Bands were visualized using Pierce ECL Western Blotting Substrate (Thermo Fisher Scientific) on X-ray films. For quantification of protein bands NIH ImageJ software was used.

Quantification of IL-1β levels in whole lung homogenates

IL-1β levels in mouse lung homogenates were quantified with a commercially available ELISA kit (Invitrogen, MA, USA) according to the manufacturer's instructions.

Detection of cell death *in situ* using terminal deoxynucleotidyl transferase dUTP nick end labeling (TUNEL) assay

For *in situ* detection of apoptosis in *Becn1*$^{+/-}$ and WT paraffin-embedded lung sections, an *in situ* cell death detection kit TMR red (Roche, Switzerland) was used as per manufacturer's instructions. Observation of cellular apoptosis was performed by detection and enumeration of TMR-labeled cells in 4-6 images per section captured at 200 × magnification.

Caspase-1 Fluorometric Activity Assay

Enzymatic activity of caspase 1 was quantified in whole lung homogenates using a caspase-1 fluorometric assay kit (R & D systems, MN, USA) according to manufacturer's instructions.

Statistical analyses

All data are presented as mean ± SEM. Statistical significance was determined by two-tailed Student's t-test for comparisons of 2 groups or one-way ANOVA followed by Tukey's post-hoc test for more than 2 groups using GraphPad Prism 7 (GraphPad Software, Inc, La Jolla, CA). $P < 0.05$ was considered significant.

References

E1. Hirakawa H, Pierce RA, Bingol-Karakoc G, Karaaslan C, Weng M, Shi GP, Saad A, Weber E, Mariani TJ, Starcher B, Shapiro SD, Cataltepe S. Cathepsin S deficiency confers protection from neonatal hyperoxia-induced lung injury. *Am J Respir Crit Care Med* 2007; 176: 778-785.

E2. Coalson JJ, Winter VT, Siler-Khodr T, Yoder BA. Neonatal chronic lung disease in extremely immature baboons. *Am J Respir Crit Care Med* 1999; 160: 1333-1346.

E3. Yoder BA, Coalson JJ. Animal models of bronchopulmonary dysplasia. The preterm baboon models. *Am J Physiol Lung Cell Mol Physiol* 2014; 307: L970-977.

E4. Coalson JJ, Winter VT, Gerstmann DR, Idell S, King RJ, Delemos RA. Pathophysiologic, morphometric, and biochemical studies of the premature baboon with bronchopulmonary dysplasia. *The American review of respiratory disease* 1992; 145: 872-881.

E5. Liang X, Gupta K, Quintero JR, Cernadas M, Kobzik L, Christou H, Pier GB, Owen CA, Cataltepe S. Macrophage FABP4 is required for neutrophil recruitment and bacterial clearance in Pseudomonas aeruginosa pneumonia. *FASEB J* 2019; 33: 3562-3574.

E6. Harijith A, Choo-Wing R, Cataltepe S, Yasumatsu R, Aghai ZH, Janer J, Andersson S, Homer RJ, Bhandari V. A role for matrix metalloproteinase 9 in IFNgamma-mediated injury in developing lungs: relevance to bronchopulmonary dysplasia. *Am J Respir Cell Mol Biol* 2011; 44: 621-630.

E7. Cataltepe S, Arikan MC, Liang X, Smith TW, Cataltepe O. Fatty acid binding protein 4 expression in cerebral vascular malformations: implications for vascular remodelling. *Neuropathol Appl Neurobiol* 2014; 41: 646-656.

E8. Ghelfi E, Yu CW, Elmasri H, Terwelp M, Lee CG, Bhandari V, Comhair SA, Erzurum SC, Hotamisligil GS, Elias JA, Cataltepe S. Fatty acid binding protein 4 regulates VEGF-induced airway angiogenesis and inflammation in a transgenic mouse model: implications for asthma. *Am J Pathol* 2013; 182: 1425-1433.

Supplemental Figure Legends

Figure E1. Representative immunofluorescence images of lung cryosections from *GFP/LC3* mice harvested at 6 h and 24 h of life demonstrating GFP puncta (autophagosomes) at 6 h but not at 24 h.

Figure E2. A. Immunoblot analysis for beclin 1 protein was performed using whole lung homogenates from mouse pups sacrificed on P5, P7, P10, and P14. **B.** Relative protein expression levels of beclin 1, normalized to ACTB, were determined by densitometry.

Figure E3. Immunoblot analysis for total ATG5 (ATG5 alone and conjugated to ATG12) and LAMP1 was performed using whole lung homogenates from mouse pups exposed to normoxia or hyperoxia (75% O_2) between P1 and P7. ACTB was used as a loading control.

Figure E4. Correlation analysis of LC3-II levels with p-AMPK (Pearson r = 0.94, $P < 0.01$) and p-S6 levels in whole lung homogenates from BPD group lungs based on densitometry values shown on Figure 3.

Figure E5. Baboons were delivered at 140 d gestation (equivalent of ~ 29-30 weeks human gestation) and sacrificed before first breath (140 d GC) or maintained on mechanical ventilation with either PRN or 100 % O_2 for 10 days. AMPK, p-AMPK, p62, LC3, and ACTB protein levels were analyzed by immunoblotting. Red frame indicated the 140 d GC sample with the highest level of AMPK activation along with the highest LC3 lowest p62 levels.

Figure E6. GFP-LC3 and SPC expression in normoxia-exposed P1 lung. Cryosections of *GFP-LC3* lungs harvested at 24h following normoxia exposure were incubated with a primary antibody against pro-surfactant protein C (SPC) followed by incubation with a secondary fluorophore-conjugated antibody (Alexa Fluor® 594 goat anti-rabbit IgG), then mounted in Vectashield (Vector Labs, Burlingame, CA, USA). A representative image is shown. White arrows indicate examples of GFP-positive and SPC-negative smooth muscle cells surrounding large airways, whereas yellow arrows indicate examples of GFP-positive and SPC-positive alveolar type II cells (AEC2s).

Figure E7. P-S6 is expressed in alveolar macrophages in baboon BPD and P5 hyperoxia-exposed murine lungs. Representative double IF images for p-S6 and CD68 on a baboon lung section with BPD (top panel) and p-S6 and GFP on *GFP-LC3* mouse lung cryosection harvested on P5

following hyperoxia exposure. White arrows indicate co-localization of p-S6 with CD68 in the baboon and GFP in the mouse lung section in alveolar macrophages. Scale bar, 25 μm.

Figure E8. Autophagy is functional in macrophages but not neutrophils in the nHILI model. A. BALF was harvested from *GFP-LC3* mice following normoxia or hyperoxia exposure between P1 and P7. Pooled BALF supernatants were normalized to total protein and subjected to SDS-PAGE followed by immunoblotting for GFP. B. Cryosections of *GFP-LC3* lungs harvested at P5 and P7 following hyperoxia exposure were incubated with a primary antibody against myeloperoxidase (MPO) followed by incubations with a secondary fluorophore-conjugated antibody (Alexa Fluor® 594 goat anti-rabbit IgG), then mounted in Vectashield (Vector Labs, Burlingame, CA, USA). A representative image from a P5 sample is shown. White arrows indicate examples of MPO-positive and GFP-negative neutrophils in the airspaces surrounded by GFP-positive AEC2s.

Figure E9. LC3 puncta co-localizes with the macrophage marker CD68 in tracheal aspirate cytospins from intubated preterm infants. A representative TA cytospin is shown. The majority of CD68-negative cells were identified as neutrophils based on Diff-Quik-staining (not shown) and do not exhibit any LC3 puncta. Scale bar, 25 μm.

TABLE E1

Antibody	Application	Manufacturer	Catalogue No.	Host	Dilution
AMPKα	WB	Cell Signaling Technology, Danvers, MA, USA	2793	Mouse	1:1000
ATG5	WB	Cell Signaling Technology, Danvers, MA, USA	8540	Rabbit	1:1000
β-actin	WB	Invitrogen, Carlsbad, CA, USA	AM4302	Mouse	1:5000
Beclin-1	WB	Cell Signaling Technology, Danvers, MA, USA	3738	Rabbit	1:1000
CD31	WB	Novus Biologicals, Centennial, CO, USA	NBP1-71663	Rabbit	1:1000
Cleaved Caspase-3	WB	Cell Signaling Technology, Danvers, MA, USA	9661	Rabbit	1:1000
FABP4	IF	Abcam, Cambridge, UK	ab13979	Rabbit	1:1000
GFP	WB	Invitrogen, Carlsbad, CA, USA	A-11122	Rabbit	1:1000
LC3	WB	Medical & Biological Laboratories Co., Japan	PM036	Rabbit	1:1000
MPO	IF	R&D Systems, Inc., Minneapolis, MN, USA	AF3667	Goat	1:100
p21	WB	Cell Signaling Technology, Danvers, MA, USA	2946	Mouse	1:1000
p62	WB	Sigma-Aldrich, St. Louis, MO, USA	P0067	Rabbit	1:1000
Phospho-AMPKα (Thr172)	WB, IF	Cell Signaling Technology, Danvers, MA, USA	2535	Rabbit	1:1000
Phospho-S6 (Ser240/244)	WB, IF	Cell Signaling Technology, Danvers, MA, USA	5364	Rabbit	1:1000
Parkin	WB	Cell Signaling Technology, Danvers, MA, USA	4211	Mouse	1:1000
PINK1	WB	Novus Biologicals,	BC100-494	Rabbit	1:1000

		Centennial, CO, USA			
Prosurfactant Protein C (SPC)	WB, IF	Abcam, Cambridge, UK	ab90716	Rabbit	1:1000
α-SMA	IF	Sigma Aldrich, St. Louis, MO, USA	A-2547	Mouse	1:500
TFEB	WB	Bethyl Laboratories, Montgomery, TX, USA	A303-673A-M	Rabbit	1:500

TABLE E2

Secondary Antibody Name	**Manufacturer**	**Catalogue No.**	**Host**	**Dilution**
Anti-Mouse IgG-HRP	Cell Signaling Technology, Danvers, MA, USA	7076	Horse	1:5000
Anti-Rabbit IgG-HRP	Cell Signaling Technology, Danvers, MA, USA	7074	Goat	1:5000

TABLE E3

Gene	**Primer Sequence (5` to 3`)**
18sRNA-F	GTAACCCGTTGAACCCCATT
18sRNA-R	CCATCCAATCGGTAGTAGCG
TNFα-F	CTTCTGTCTACTGAACTTCGGG
TNFα-R	CAGGCTTGTCACTCGAATTTTG
IL-1β-F	ACGGACCCCAAAAGATGAAG
IL-1β-R	TTCTCCACAGCCACAATGAG
IL-18-F	GCCTCAAACCTTCCAAATCAC
IL-18-R	GTTGTCTGATTCCAGGTCTCC
CD68-F	TACAATGTGTCCTTCCCACAGGCA
CD68-R	AGGTCAAGGTGAACAGCTGGAGAA
CXCL1-F	AACCGAAGTCATAGCCACAC
CXCL1-R	CAGACGGTGCCATCAGAG
IL-6-F	CAAAGCCAGAGTCCTTCAGAG
IL-6-R	GTCCTTAGCCACTCCTTCTG

Figure E1

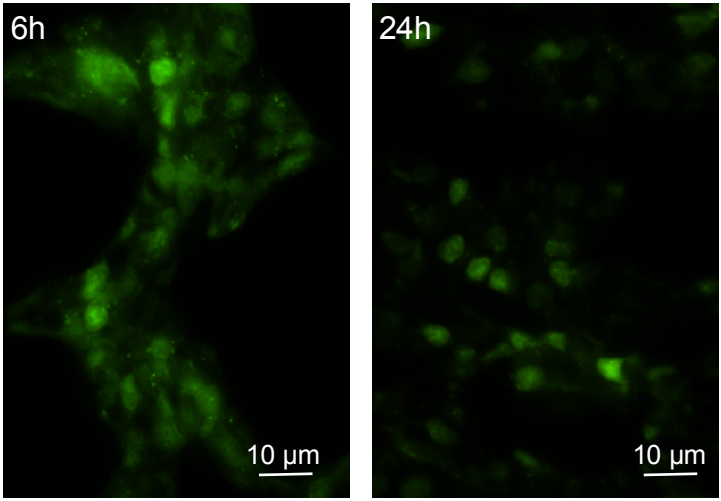

FIGURE E2

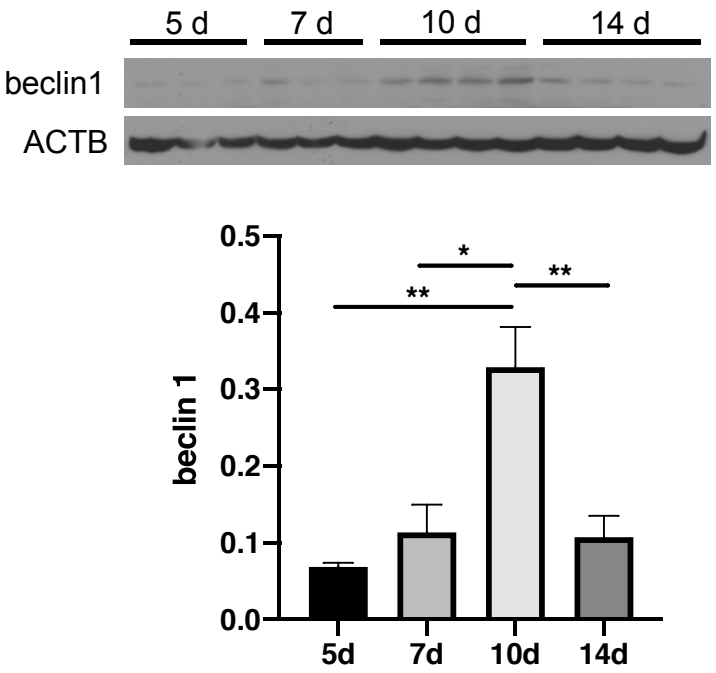
5 d
7 d
10 d
14 d
beclin1
ACTB
beclin 1
0.5
0.4
0.3
0.2
0.1
0.0
*
**
**
5d
7d
10d
14d

Figure E3

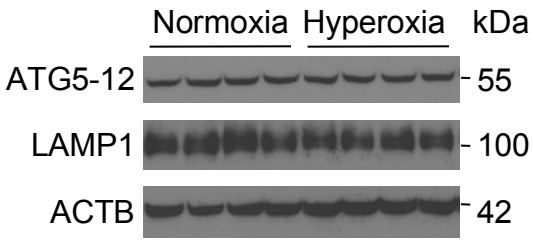

Figure E4

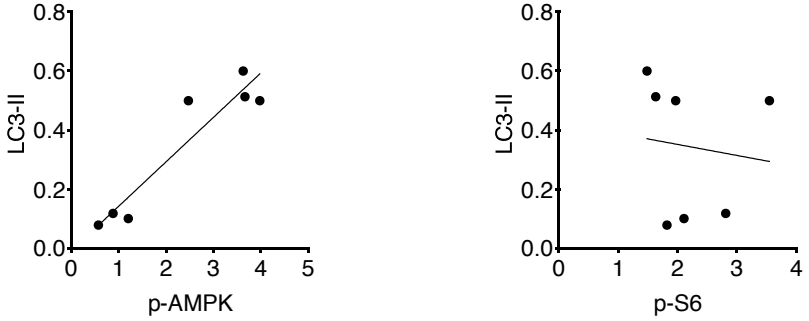

Figure E5

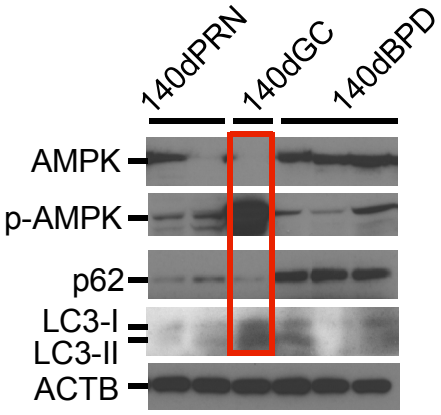

FIGURE E6

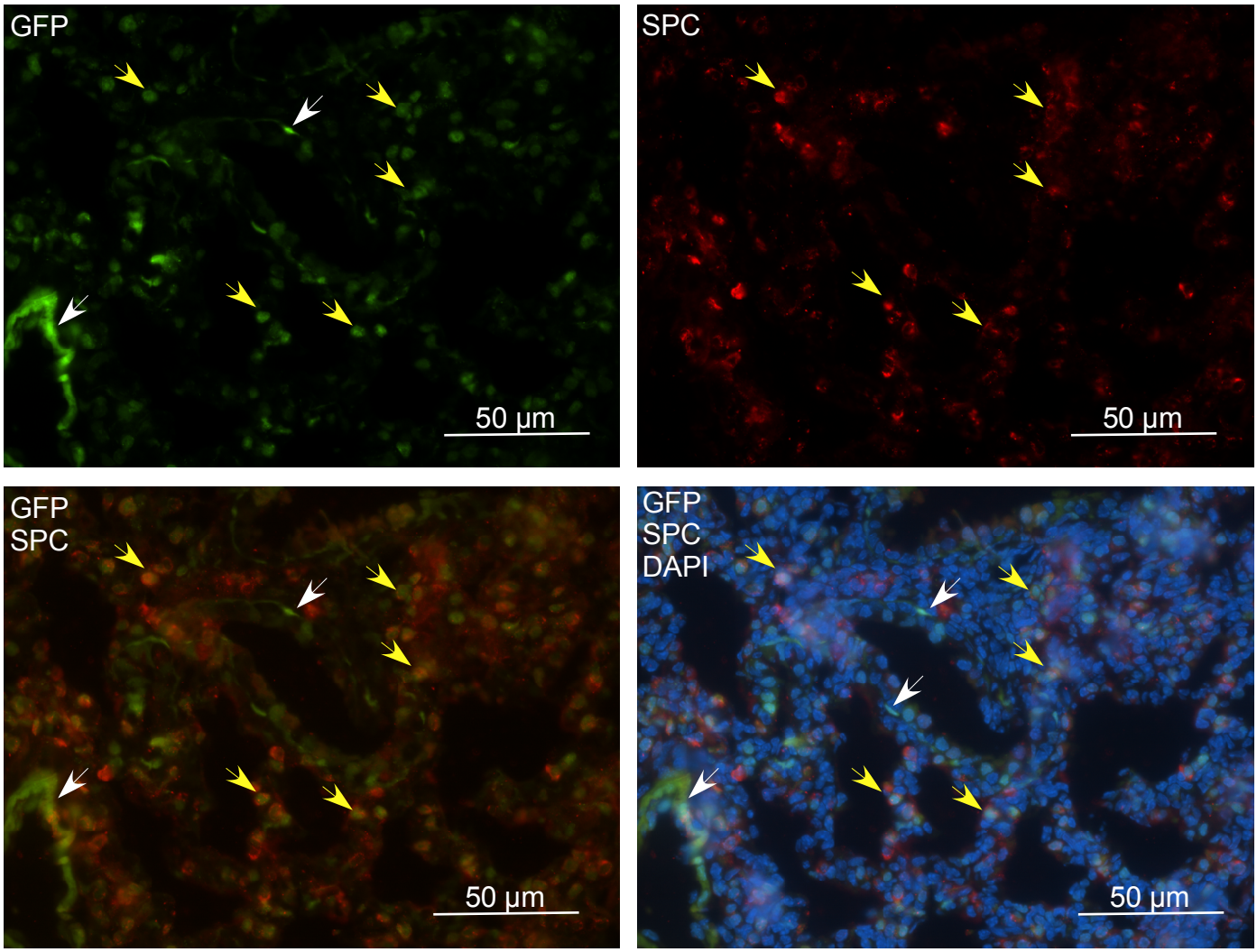

FIGURE E7

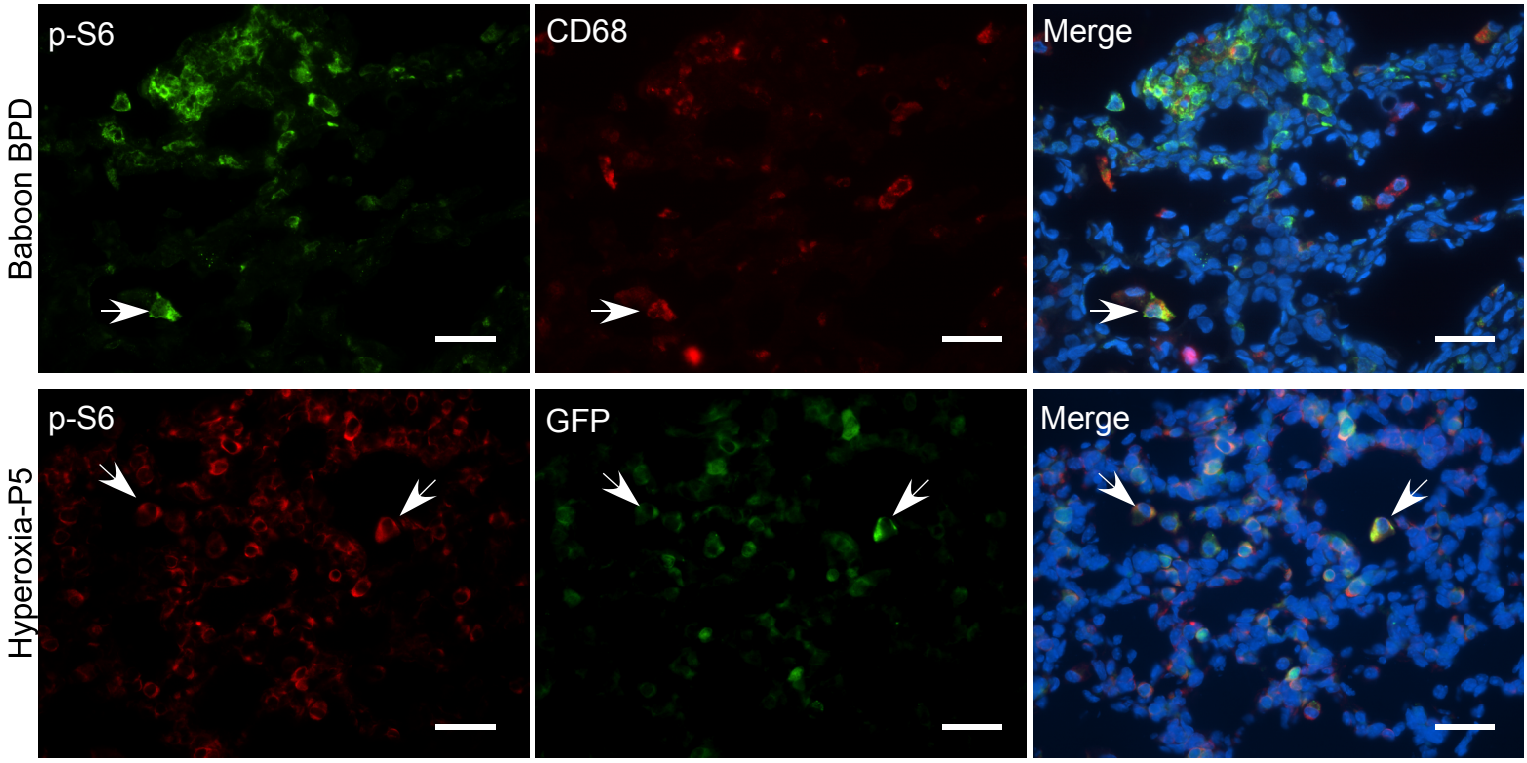

Figure E8

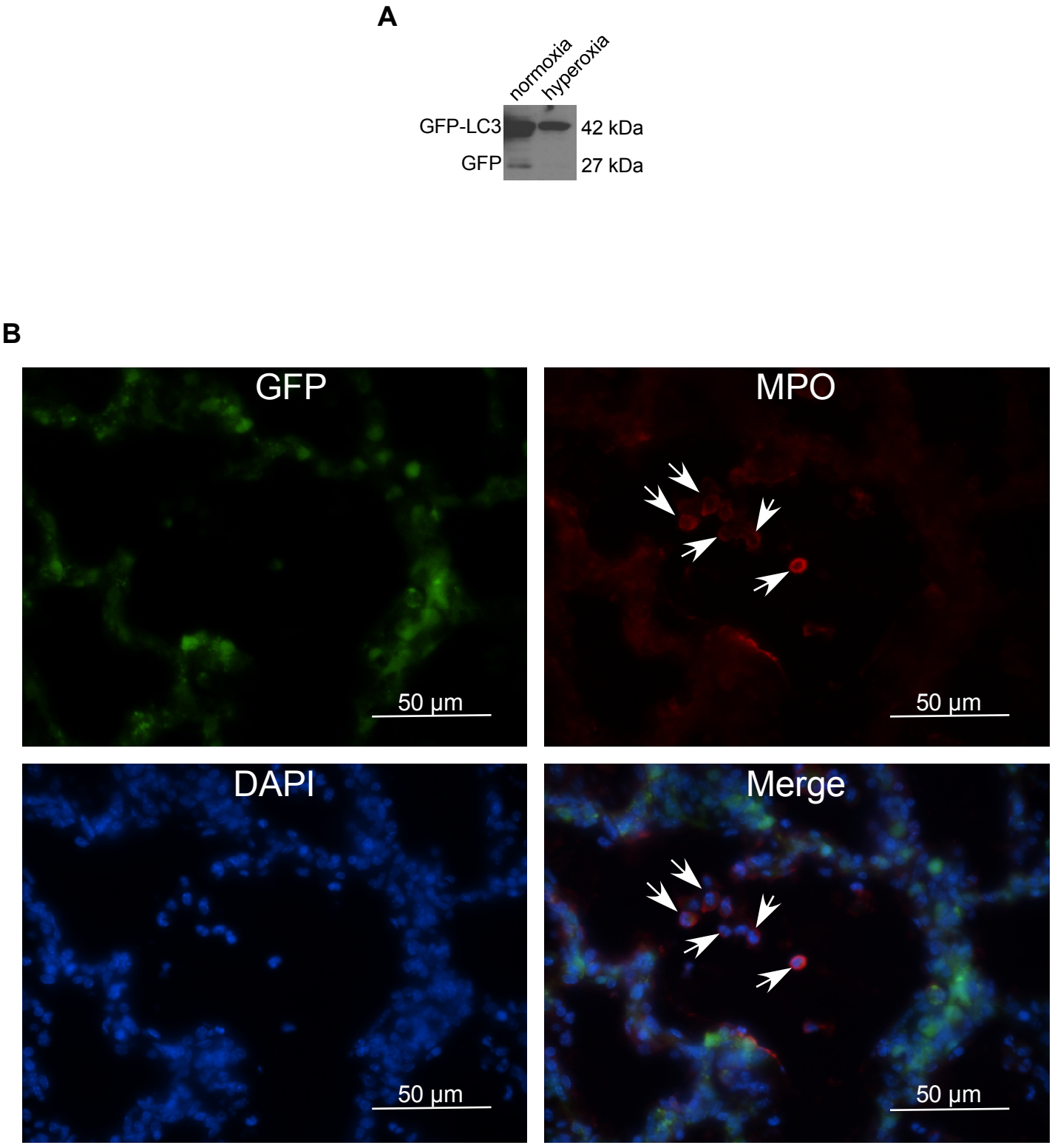
A
normoxia
hyperoxia
GFP-LC3
GFP
42 kDa
27 kDa
B
GFP
MPO
DAPI
Merge
50 μm
50 μm
50 μm
50 μm

FIGURE E9